

## Recognition of sugarcane orange and brown rust through leaf image processing

Isabela Ordine Pires da Silva Simões<sup>a,\*</sup>, Rodrigo Greggio de Freitas<sup>a</sup>, Danilo Eduardo Cursi<sup>b</sup>, Roberto Giacomini Chapola<sup>c</sup>, Lucas Rios do Amaral<sup>a</sup>

<sup>a</sup> Universidade Estadual de Campinas, Faculdade de Engenharia Agrícola (FEAGRI), Barão Geraldo 13083-875, Av. Cândido Rondon, 501, Campinas, SP, Brasil

<sup>b</sup> Centro de Tecnologia Canavieira (CTC), Fazenda Santo Antônio, s/n - Bairro Santo Antônio 13400-970 Piracicaba, SP, Brasil

<sup>c</sup> Rede Interuniversitária para o Desenvolvimento do Setor Sucroenergético (RIDES), Rodovia Anhanguera, s/n – Jardim Europa 13600-970 Araras, SP, Brasil

### ARTICLE INFO

Editor: Spyros Fountas

**Keywords:**

Phenotyping  
Disease resistance  
Object-based  
Image processing

### ABSTRACT

In experimental fields, scientists assess the resistance to orange and brown rust of sugarcane exclusively by identifying and grading infection by visual estimation on the leaves. This is time-consuming and may deliver subjective evaluations, limiting phenotyping experiments. Thus, to facilitate the leaf disease identification process, the goal of this study was to test an image analysis approach to differentiate the two types of rust on sugarcane leaves. Radial Support Vector Machine (SVM) models showed high accuracy ( $>0.88$ ) in identifying the two types of rust, classifying segments of RGB images of infected leaves generated with object-based image analysis (OBIA) segmentation. This provides a basis for the development of applications that identify the two types of rust automatically through RGB images of sugarcane leaves.

### Introduction

Two of the main diseases that affect sugarcane are orange rust, caused by the fungi *Puccinia kuehnii*, and brown rust, caused by *P. melanocephala*. Their main symptom is the appearance of spots on the leaf blade, which evolve to pustules on the lower leaf blade, which cause plant tissue death and reduction of photosynthetic area and, consequently, reduction in stalk production [1].

The main control measure against these pathogens is the use of resistant varieties [2]. Thus, one of the steps with great focus in the phenotyping process of sugarcane genetic improvement programs is the evaluation of resistance to these diseases. The estimation of the degree of infection of the leaves and the identification of the type of rust are visually made by specialists, which is always subject to the experience of the evaluator and can be affected over time, impairing the repeatability of the observations [3].

Identifying the type of rust is a complex task when performed by specialists with the naked eye, but when observed with a magnifying glass or very high-resolution image, the differences in color and shape of the first pustules are more easily observed (Fig. 1). Orange rust has smaller pustules, appearing orange or orange-brown in color, which do not turn dark over time. On the other hand, Brown rust has larger and

more elongated pustules, appearing orange and reddish-brown in color, becoming dark brown when mature [4]. Some studies were dedicated to the recognition of rust in RGB images of sugarcane leaves, among other diseases [5]. However, no study aimed to distinguish the symptoms between the two types of rust.

Therefore, this work hypothesizes that the differentiation between the symptoms of the two types of rust in the images of the leaves is given mainly by the characteristics of color, shape, and texture of the images of the pustules.

Image processing has been applied in the recognition of many diseases in plants [5–7]. The accuracy of image-based recognition for plant diseases depends heavily on the segmentation of lesions in the images [8]. Threshold-based image segmentation methods have been widely used in image segmentation of diseased plant lesions [6]. However, there is usually a high color variation, both between lesions from different diseases and between lesions of a disease at different stages. Therefore, it is very difficult to determine the appropriate threshold when threshold-based image segmentation methods are used to solve segmentation problems for plant disease images with complex colors. In this study, we tested automatic object-oriented segmentation, which eliminates the need to establish spectral thresholds for segmentation and therefore eliminates human bias from processing. Object-oriented image

\* Corresponding author.

E-mail address: [isaopssimoes@gmail.com](mailto:isaopssimoes@gmail.com) (I. Ordine Pires da Silva Simões).



analysis (OBIA) is widely used in conventional remote sensing image processing (aerial and satellite images), but as far as we know, it has not yet been tested for image analysis of leaf diseases.

Furthermore, we proceeded with the extraction and selection of predictive characteristics of the classes of the segments collected and classification of these by machine learning models. Based on selected predictive features, disease recognition models were built using three supervised learning methods, including random forest (RF), support vector machine (SVM), and K-nearest neighbor (KNN). Therefore, the objective of this study was to develop a methodology to identify the symptoms of the two types of sugarcane rust through the processing of RGB images of the leaves. With this, we hope to provide a basis for the development of an automatic diagnosis system.

## Material and methods

A sugarcane phenotyping experimental field composed by 24 developing varieties in the São Paulo State, Brazil (coordinates 22°18'58.33"S; 47°22'50.02"O) was the study site. The plants were naturally infected through the donation of spores from susceptible varieties to orange and brown rust planted as spreader rows into the experimental area. Ninety sugarcane leaves were collected throughout the experiment at 195 days after planting, when there were proper humidity and temperature for rust development (high humidity and temperature, from 29 to 34°). So infected leaves with different ages were found in different stages of the diseases, allowing the evaluation of symptoms with varied shades. The processing leaf images proposed here was an object-oriented segmentation, followed by automatically extracting characteristics from the segments and classifying them by a machine learning model. An expert performed a naked-eye evaluation of the diseases in each leaf. Such classification was compared to the automatically classification through image analysis.

## Image acquisition and processing

The images of the infected leaves were obtained with a size of 3872 × 2592 pixels (Raw + Jpeg formats) with an RGB digital camera with a resolution of 10.2 megapixels in a partially covered environment with diffused natural lighting, totaling 90 images. A 0.30 m longboard with a white background was made to obtain images of the same size, covering the middle third of the leaves and pressing them to make them as expanded as possible. The positioning of the camera lens was parallel to the plane of the leaves (nadir) and 0.35 m away from them.

The methodological strategy for processing leaf images proposed in this work is an object-oriented segmentation [9–12], followed by automatically extracting characteristics from the segments and classifying them by a machine learning model without establishing spectral thresholds for segmentation and therefore eliminating human bias from processing. The proposal is that the method allows the identification of each type of rust. For such, we tested three algorithms: random forest (RF), support vector machine (SVM), and K-nearest neighbor (KNN). Regarding SVM, the kernels of the polynomial and radial basis function (RBF) are the most commonly used functions for classification by SVM [13]; several studies have found that RBF is superior to the polynomial kernel for classifying remote sensing data [14]. Therefore, we used the SVM models with a radial basis function. The classification models were developed using the “caret” package within the R software version 3.5.3.

The image processing and analysis workflow is shown in Fig. 2 and the steps are described in the following items.

The color of the leaves varies significantly with the stage of development, senescence, and variety of the crop. For this reason, image filtering techniques are insufficient to minimize the effect of this variation when the objective is to use an automatic processing method and not individual analyzes for each image of the leaves. Considering this variation, for the classification models to be trained, sub-images with parts of healthy leaves with different shades and lesions in all stages of

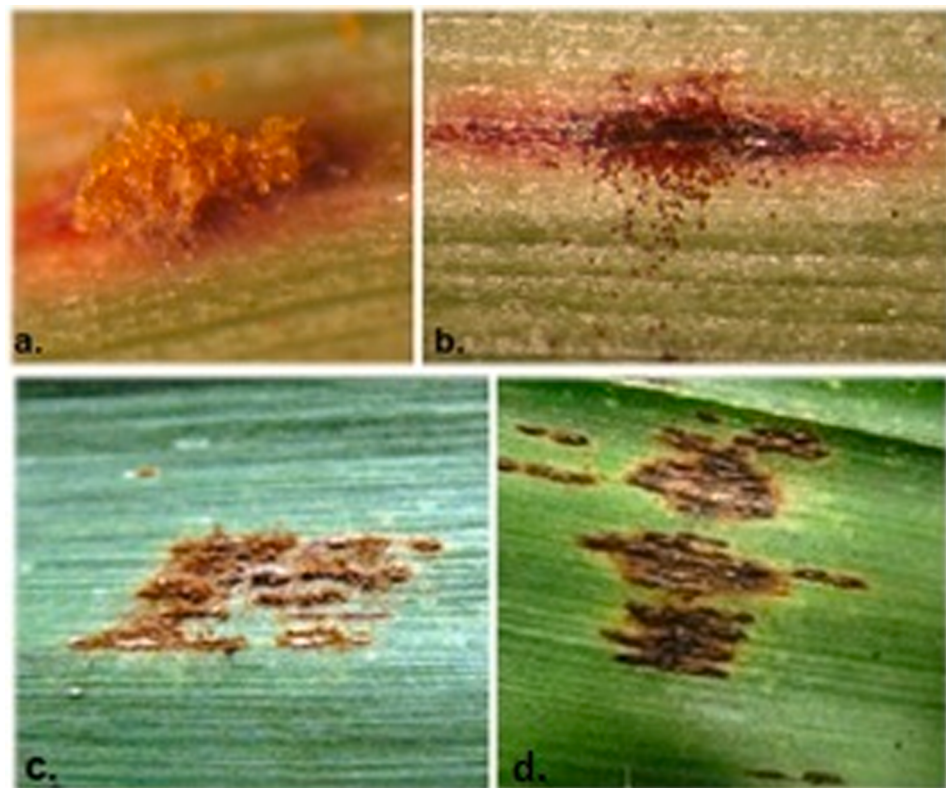


**Fig. 1.** (a) High-resolution orange rust pustule; (b) High-resolution brown rust pustule; (c) Orange rust pustules, and (d) Brown rust pustules with a lower resolution [4].

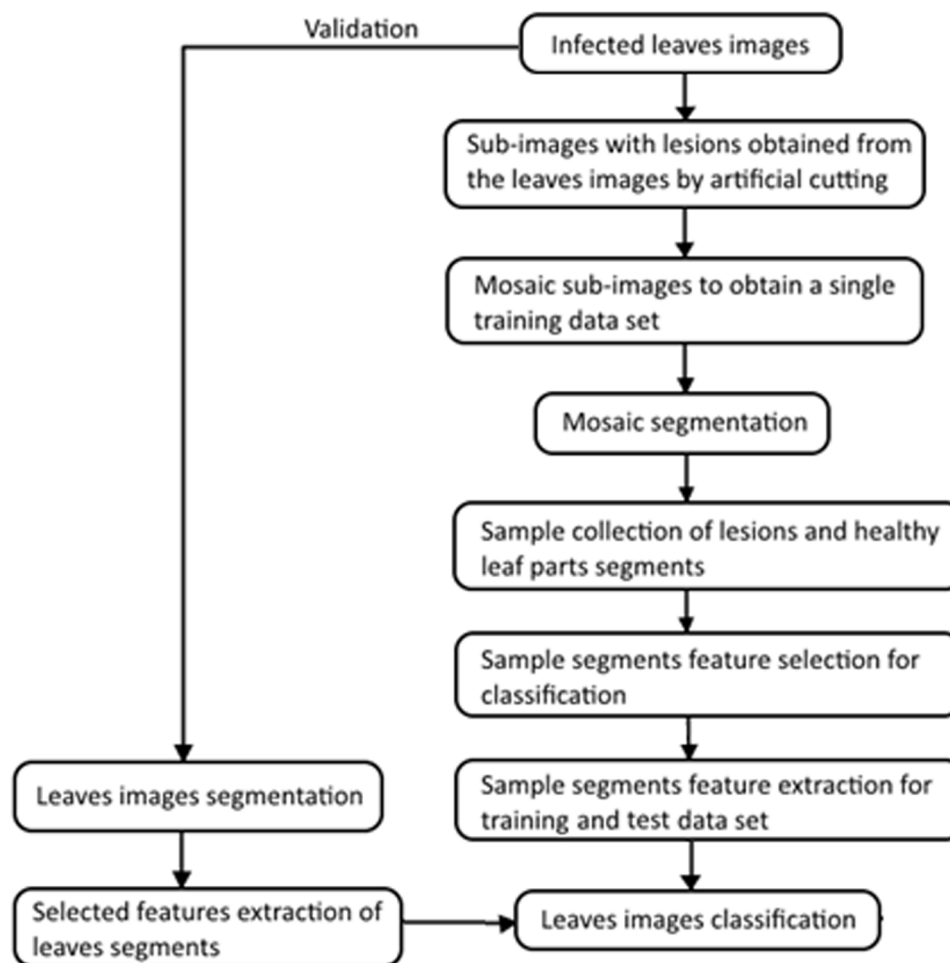


**Fig. 2.** Workflow diagram of the main steps for processing and analyzing leaf images.

development from both rusts were extracted by artificial cutting of the entire images of the leaves (Fig. 3). In total, we obtained 216 sub-images with one or multiple lesions typical of orange rust and 217 sub-images with lesions of brown rust. The sub-images were then mosaiced in Jpeg format. After segmenting the mosaics, which will be detailed in the next section, samples of lesion segments and healthy leaves were simultaneously collected to generate data files to be used in the training and testing of the classification models. In all, 1039 segments of orange rust lesions, 497 of brown rust, and 1972 of healthy leaf lesions were sampled in the image mosaic.

#### Validation of the disease identification method

For validation of the machine learning models, images of ten other leaves were segmented, and samples of lesion and healthy leaf segments were collected. 762 lesion segments were obtained from orange rust, 443 from brown rust, and 1886 from healthy leaf for the validation dataset. Data on the selected characteristics of the segments were then extracted so that they could be classified by the models.

#### Segmentation

Commercial software eCognition Developer 8 (Trimble GeoSpatial, Munich, Germany), widely used in remote sensing image processing, was used for object-oriented image segmentation with the multi-resolution segmentation algorithm [15]. The appropriate segmentation scale was set at 10 to generate the segments that best delimited the lesion areas. The values of the other parameters involved in the

segmentation were 1 for the weight of all bands, 0.1 for format, and 0.5 for compactness. Before segmentation, we also generate the conversion of the RGB color space to HSI (Hue, Saturation, Intensity) to minimize the effects of lighting variation and obtain color characteristics (Hue) of the image elements, important for the segmentation of RGB images and consequently to separate the classes of interest from the segments [16].

#### Selection of segment characteristics

After segmentation and collection of lesion samples from the two rusts and healthy leaf, the feature space optimization function was applied, which offers a method to calculate, mathematically, the best combination of features for differentiation or the greatest mean minimum distance between samples of classes of interest [17]. Initially, the features were selected from a set of 202 color, shape, and texture features available in the software, and of these, 114 were selected, and then training and testing of the classification models were performed. In an attempt to simplify the models, the texture features were removed, and a set of 52 spectral and format features available in the software was optimized, resulting in 25 main features for differentiating the samples collected in the images, resulting in better classifications, therefore, they were adopted in the remainder of the study. The characteristics and the position in the ranking of importance for differentiating the classes of interest (orange and brown rust and healthy leaf) are found in Table 1. The description of these same characteristics is found in Table 2.

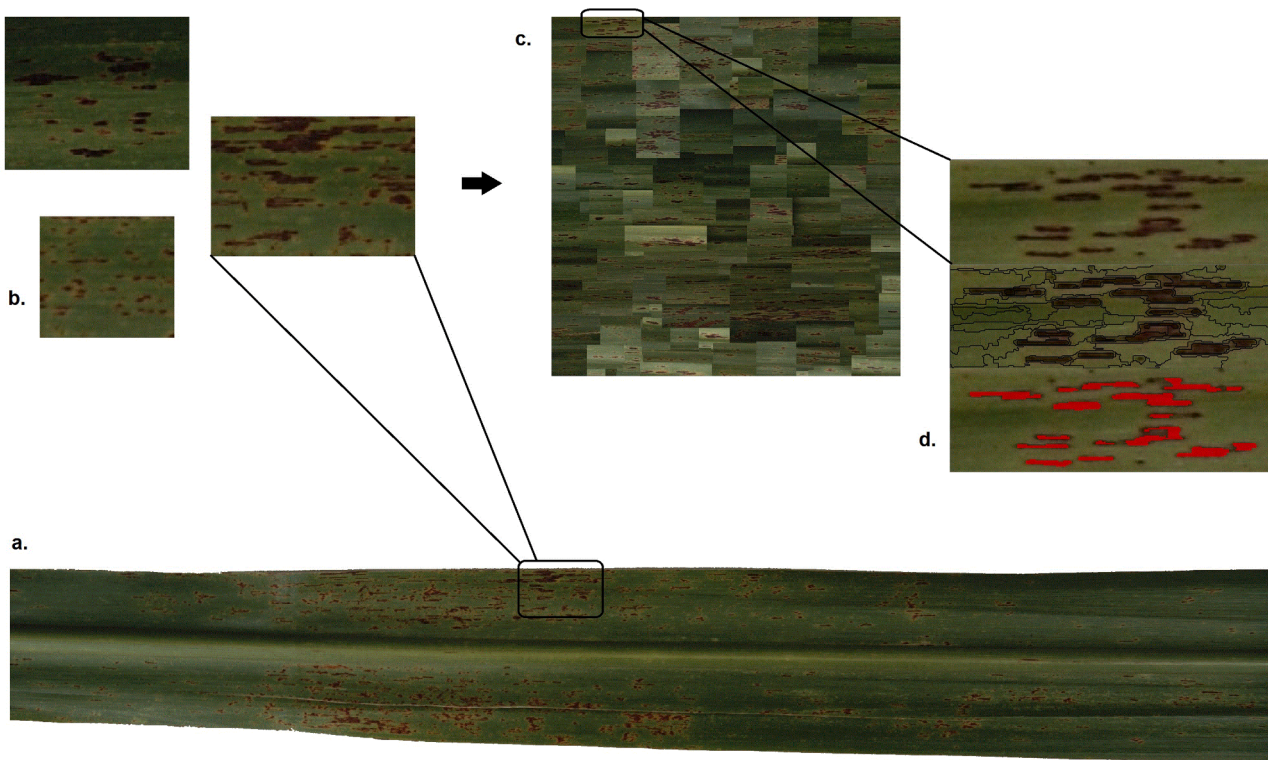


**Fig. 3.** Image preparation scheme for data collection for training and testing the classification models: (a) entire 30 cm image of a sugarcane leaf infected with orange rust; (b) examples of sub-images with lesions; (c) mosaic of sub-images of lesions and healthy leaf with different shades; (d) example of a segmented mosaic area with a subsequent sampling of lesion segments and healthy leaf.

**Table 1**  
Features extracted from the segments and classification of importance.

Feature importance classification	Feature	Feature importance classification	Feature
1	Number of edges (polygon)	14	Degree of skeleton branching
2	Mean Layer 1*	15	Rectangular Fit
3	Max. diff.	16	Brightness
4	Standard deviation Layer 1*	17	Standard deviation of area represented by segments
5	Average area represented by segments	18	Mean Layer 2
6	Radius of largest enclosed ellipse	19	Standard deviation of length of edges (polygon)
7	Compactness (polygon)	20	Roundness
8	Standard deviation Layer 3*	21	Radius of smallest enclosing ellipse
9	Elliptic Fit	22	Mean Layer 3*
10	Standard deviation Layer 2*	23	Compactness
11	HIS Transformation Hue	24	Length
12	Density	25	Shape index
13	Average length of edges (polygon)	–	–

\* Layer 1 = Red, Layer 2 = Green, Layer 3 = Blue.

#### Accuracy assessment

In this study, accuracy was the statistic used to evaluate the classification models (Eq. (1)).

$$\text{Accuracy} = \frac{\text{Number of correct predictions}}{\text{Total number of predictions}} \quad (1)$$

Balanced confusion matrices for three-class problems were used to assess the accuracy of the classifications [18]. Overall accuracy denotes the probability that a randomly selected sample will be correctly classified according to its label class.

The dataset was randomly divided into 70% for the training set and 30% for the test set. The k-fold cross validation was used to adjust the parameters in the model training stage. In this study, cross-validation with four folds with two repetitions was used. After training, test samples were used for accuracy assessment.

The Kappa coefficient ( $K_c$ ), which is also a measure of classification accuracy, was calculated as follows (Eq. (2)) [19]:

$$K_c = N \sum_{n=1}^r \frac{n_{irow} n_{icol}}{N^2} - \sum_{i=1}^r n_{irow} n_{icol} \quad (2)$$

where  $n_{irow}$  is the  $i$ th row and  $i$ th column position element,  $n_{icol}$  are the column sums, and  $n_{irow}$  are the row sums. A Kappa value of 1 represents a perfect agreement, while a value of 0 represents no agreement.

#### Results

The models were able to differentiate the two types of rust with high accuracy (Table 3 – accuracy > 0.8), both for the test and validation data sets. These results show the models were not over fitted.

Considering the accuracy of disease recognition with the validation dataset, the best model built was with radial SVM based on the 9 main predictive characteristics selected. The importance of the main characteristics of the segments for the differentiation of diseases by the models is shown in Fig. 4. Removing the remaining features for training the models did not change the classification accuracy of the models. Therefore, we can highlight that based on these 9 characteristics,

**Table 2**

Features extracted from segments and definitions [15].

Feature	Definition
Number of edges (polygon)	The number of edges of a polygon.
HIS Transformation Hue	Hue (color)
Average area represented by segments	The average area of all triangles created by a Delaunay triangulation.
Elliptic Fit	Describes how well an image object fits into an ellipse of similar size and proportions.
Density	Describes the distribution in space of the pixels of an image object.
Average length of edges (polygon)	The average length of all edges in a polygon.
Radius of smallest enclosing ellipse	Describes how much the shape of an image object is similar to an ellipse.
Max. diff.	<ul style="list-style-type: none"> <li>• <math>i, j</math> are image layers</li> <li>• <math>\bar{c}(v)</math> is the brightness of image object <math>v</math></li> <li>• <math>\bar{c}_{i(v)}</math> is the mean intensity of image layer <math>i</math> of image object <math>v</math></li> <li>• <math>\bar{c}_{j(v)}</math> is the mean intensity of image layer <math>j</math> of image object <math>v</math></li> <li>• <math>c_k^{max}</math> is the brightest possible intensity value of image layer <math>k</math></li> <li>• <math>K_B</math> are image layers of positive brightness weight with <math>K_B = fk \cdot 2K: wk = 1g</math>; where <math>wk</math> is the image layer weight.</li> <li>• <math display="block">\frac{1}{K_B} c_k^{max} = \frac{\max_{i, j \in K_B}  \bar{c}_{i(v)} - \bar{c}_{j(v)} }{\bar{c}(v)}</math></li> </ul>
Rectangular Fit	Describes the difference between a master rectangle and the considered object using the same measure of area, width and length for the master rectangle.
Length	The length of a 2D image object is calculated using the length-to-width ratio.
Compactness (polygon)	The ratio of the area of a polygon to the area of a circle with the same perimeter.
Standard deviation of length of edges (polygon)	Measures how the lengths of edges deviate from their mean value.
Radius of largest enclosed ellipse	Describes how similar an image object is to an ellipse.
Standard deviation of area represented by segments	The standard deviation of all triangles created by the Delaunay triangulation.
Standard deviation Layer 1/2/3*	For each image layer, a separate standard deviation feature.
Mean Layer 1/2/3*	The mean intensity of all pixel/voxels forming an image object.
Shape index	Describes the smoothness of the image object borders.
Degree of skeleton branching	The internal structure of the polygons can be derived using skeletons. A very high degree of skeleton branching is an indication of a complex and non-smooth polygon shape.
Compactness	Can be defined by the product of the width and the length over pixels numbers.
Brightness	Best image layers providing the spectral information are used for calculation. It is the mean intensity of the image layer of the image object.
Roundness	Describes how similar an image object is to an ellipse. It is calculated by the difference of the enclosing ellipse and the enclosed ellipse.

\* Layer 1 = Red, Layer 2 = Green, Layer 3 = Blue.

machine learning models, such as those tested in this study, are able to recognize the lesions of both types of rust in RGB images of infected leaves through object-oriented segmentation. The color values (Hue), obtained with the transformation of the HIS color space, was the most important predictive feature for the classification.

## Discussion

The complexity of analyzing plant disease images presents major challenges for segmentation and classification [8]. Image processing has been widely used in the analysis of foliar diseases, with the segmentation of injured areas being one of its most important phases. Image

**Table 3**

Results of model classification for sugarcane orange and brown rust using the three machine learning algorithms based on 25 characteristics of leaf image segments for test and validation datasets.

Accuracy of testing set (%)	RF	KNN	SVM radial	
Overall accuracy (%)	90.0	89.0	89.0	
Balanced accuracy (%)	Orange Brown Healthy leaf	83.0 85.0 99.0 80.0	83.0 82.0 99.0 79.0	84.0 81.0 99.0 80.0
Kappa				
Accuracy of validation set (%)	RF	KNN	SVM radial	
Overall accuracy (%)	90.0	89.0	90.0	
Balanced accuracy (%)	Orange Brown Healthy leaf	87.0 80.0 98.0	86.0 76.0 98.0	88.0 80.0 99.0
Kappa				
	81.0	79.0	82.0	

segmentation methods based on spectral thresholds are widely used in image segmentation of leaf lesions [20]. However, there is great variation in color, both between lesions of different diseases and between lesions at different stages of infection, in addition to a great variation among the several green shades present in healthy leaf areas, which usually requires the determination of individual threshold for each leaf analyzed [8]. Thus, it is difficult to determine the appropriate thresholds for satisfactory segmentation when there is a complex range of colors. In addition, filters can be applied according to the image quality of each leaf. Therefore, the method proposed in this work with object-oriented segmentation (OBIA) can be further explored, aiming to simplify the recognition of several diseases, inserting this theme more in the large area of remote sensing. Differentiation between lesions and areas of healthy leaf is more easily done on the basis of color characteristics, although for many diseases of different crops, symptoms often do not have well-defined borders [8]. The segmentation method (OBIA) allows for standardization in the delimitation of areas of infection, reducing the error in classification.

In this study, 202 features of color, shape, and texture were extracted and tested, of which 114 were initially selected according to their importance for separating the classes of interest from the segmented objects. The texture features were removed from the set of predictive variables since they proved to be redundant for the recognition of the classes (orange rust, brown rust, and healthy leaf), thus leaving 52 color and shape characteristics. Of these, 25 main features were selected through the optimization function.

These 25 selected features then served as predictive variables for training, testing and validating the machine learning models. Satisfactory classification results were also obtained with disease recognition models built based on only 9 features selected as most important by the models, indicating that these could be used effectively for the identification of the two diseases, as well as the distinction between diseased parts and health of sugarcane leaves. With the transformation in the color space to HSI, it was possible to satisfactorily differentiate the symptoms with the color characteristics (Hue), the maximum difference (Max. Diff.) (Table 2), the standard deviation of reflection intensity in the three bands (RGB), the average reflection intensity of the segments also in the 3 bands, and the brightness segments value ( $I$  in HSI). In other words, the distinction between the symptoms of the two diseases and between these and healthy leaf segments was based on color and intensity features and not on shape or texture characteristics.

The attempt to recognize the diseases through RGB image processing of the leaves generated satisfactory results, with no great confusion in the distinction between the two types of rust or between these and healthy leaf areas. The results showed that the recognition power was similar for the three machine learning algorithms employed, but radial SVM deliverer an overall better result. The classification accuracy of the diseases of the validation set was very close to that of the test set, which indicated that this model could not only be used to obtain satisfactory recognition results but also has a generalization ability, providing a basis

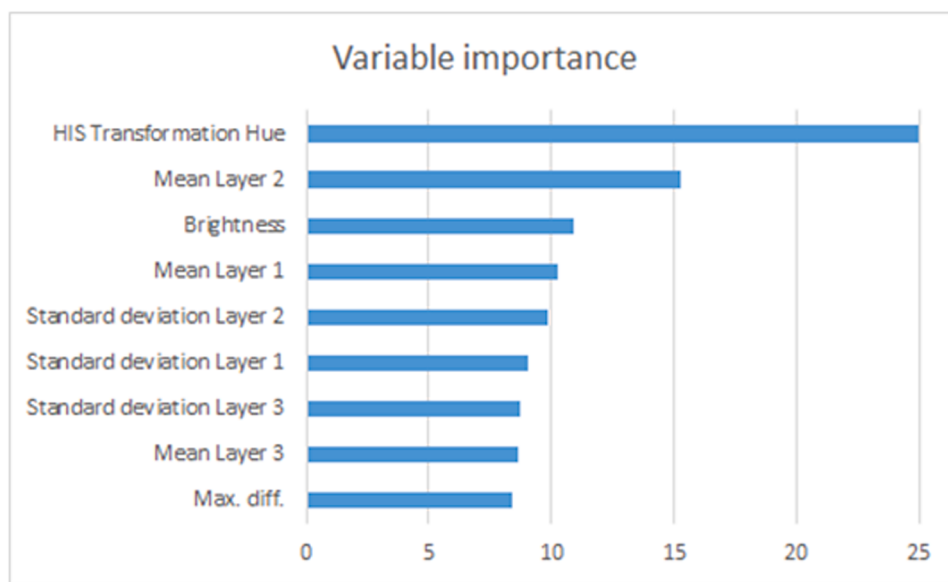


**Fig. 4.** Importance of the main 9 features selected by the machine learning models among the 25 features selected after segmentation and labeling of the samples used to generate the models.

for building an automatic disease diagnosis system in RGB images of sugarcane leaves.

The complex background of images acquired in the field presents great challenges for segmentation and recognition of targets in the images [8]. The images of the sugarcane leaves used in this study were taken on a white background. Therefore, further studies are needed to determine whether the methods used in this study are suitable for the automatic identification and diagnosis of leaf diseases as it is in the field.

In this study, we investigated the recognition of two of the main diseases evaluated in the phenotyping of new sugarcane varieties for the genetic improvement process. It would be interesting to build a comprehensive pattern database of lesion images to establish solid foundations for the application of the technology for automatic recognition of other crop diseases in leaf images. Currently, the use of smartphones to take pictures and process data has become an important tool [21]. A mobile application could be developed using the ideal image recognition model of sugarcane leaf diseases built in this study to diagnose and share information [22]. Once implemented, this process would not require specialized personnel or any chemical reagents.

## Conclusion

With the object-oriented segmentation of RGB images of sugarcane leaves infected by orange and brown rust and transformation in the color space for HSI, it was possible to satisfactorily differentiate the symptoms of the two types of rust, orange and brown.

Disease recognition models were constructed using three supervised learning methods: RF, radial SVM, and KNN. Better classification performance was obtained with the radial SVM model generated based on the 9 main predictive features selected.

Recognition of plant diseases requires specialized and experienced technical personnel to carry out visual evaluation about rust infestation on sugarcane varieties been experimented in phenotyping trials. Thus, a large amount of human and material resources is usually required. Therefore, a viable solution was provided to diagnose and identify the two types of sugarcane rust through RGB images of infected leaves.

## Declaration of Competing Interest

The authors declare that they have no known competing financial interests or personal relationships that could have appeared to influence

the work reported in this paper.

## Data availability

Data will be made available on request.

## Acknowledgments

We gratefully acknowledge the Interuniversity Network for the Development of the Sugarcane Industry in Brazil – RIDESA general manager Hermann Paulo Hoffmann and field technicians for their support in the experiment.

## Funding

This study was financed in part by the Coordenação de Aperfeiçoamento de Pessoal de Nível Superior – Brasil (CAPES) – Finance Code 001.

## References

- [1] S. Sanjel, B. Chaulagain, I.M. Small, J.C. Comstock, M. Hincapie, R.N. Raid, P. Rott, Comparison of progress of brown rust and orange rust and conditions conducive for severe epidemic development during the sugarcane crop season in Florida, *Plant Dis.* 103 (5) (2019) 825–831, <https://doi.org/10.1094/PDIS-05-18-0862-RE>.
- [2] M. Dal-Bianco, M.S. Carneiro, C.T. Hotta, R.G. Chapola, H.P. Hoffmann, A.A. F. Garcia, G.M. Souza, Sugarcane improvement: How far can we go? *Curr. Opin. Biotechnol.* 23 (2) (2012) 265–270, <https://doi.org/10.1016/j.copbio.2011.09.002>.
- [3] C.H. Bock, P.E. Parker, A.Z. Cook, T.R. Gottwald, Visual Rating and the Use of Image Analysis for Assessing Different Symptoms of Citrus Canker on Grapefruit Leaves, *Plant Dis.* 92 (4) (2008) 530–541, <https://doi.org/10.1094/PDIS-92-4-0530>.
- [4] J.T. Ferrari, R. Harakava, R.J. Domingues, I.M.L. Terçariol, J.G. Töfli, Ferrugem alaranjada da cana-de-açúcar no Brasil, *Biológico* 75 (2013) 71–74.
- [5] R. Manavalan, Efficient Detection of Sugarcane Diseases through Intelligent Approaches : A Review, *Asian J. Res. Rev. Agricult.* 3 (4) (2021) 27–37.
- [6] F. Qin, D. Liu, B. Sun, L. Ruan, Z. Ma, H. Wang, Identification of alfalfa leaf diseases using image recognition technology, *PLoS One* 11 (12) (2016) 1–26, <https://doi.org/10.1371/journal.pone.0168274>.
- [7] S. Srivastava, P. Kumar, N. Mohd, A. Singh, F.S. Gill, A Novel Deep Learning Framework Approach for Sugarcane Disease Detection, *SN Comp. Sci.* 1 (2) (2020) 1–7, <https://doi.org/10.1007/s42979-020-0094-9>.
- [8] J.G.A. Barbedo, A review on the main challenges in automatic plant disease identification based on visible range images, *Biosyst. Eng.* 144 (2016) 52–60, <https://doi.org/10.1016/j.biosystemseng.2016.01.017>.

- [9] T. Blaschke, Object based image analysis for remote sensing, *ISPRS J. Photogramm. Remote Sens.* 65 (1) (2010) 2–16, <https://doi.org/10.1016/j.isprsjprs.2009.06.004>.
- [10] A. Jaklic, A. Leonards, F. Solina, Segmentor - An object-oriented framework for image segmentation, in: *Proceedings of 3rd Slovenian-German and 2nd SDRV Workshop, 1996*, pp. 331–340.
- [11] B.A. Johnson, L. Ma, Image segmentation and object-based image analysis for environmental monitoring: Recent areas of interest, researchers' views on the future priorities, *Rem. Sens.* 12 (11) (2020), <https://doi.org/10.3390/rs12111772>.
- [12] Y. Zhang, T. Maxwell, A fuzzy logic approach to supervised segmentation for object-oriented classification, *Am. Soc. Photogrammet. Rem. Sens.* 3 (1) (2006) 1706–1716.
- [13] H. Ye, W. Huang, S. Huang, B. Cui, Y. Dong, A. Guo, Y. Jin, Identification of banana fusarium wilt using supervised classification algorithms with UAV-based multi-spectral imagery, *Int. J. Agric. Biol. Eng.* 13 (3) (2020) 136–142, <https://doi.org/10.25165/j.ijabe.20201303.5524>.
- [14] X. Yang, Parameterizing Support Vector Machines for Land Cover Classification, *Photogrammet. Eng. Rem. Sens.* 77 (1) (2011) 27–37.
- [15] Definiens. (2012). Definiens Developer XD 2.0.4 Reference Book, 106. Retrieved from [www.definiens.com](http://www.definiens.com).
- [16] S. Raut, K. Ingole, Review On Leaf Disease Detection Using Image Processing Techniques, *Int. Res. J. Eng. Tech. (IRJET)* 4 (4) (2017) 22–24.
- [17] Trimble Inc. (2017). eCognition Developer 9.1, (March). Retrieved from <http://www.ecognition.com>.
- [18] Grandini, M., Bagli, E., & Visani, G. (2020). Metrics for Multi-Class Classification: an Overview, 1–17. Retrieved from <http://arxiv.org/abs/2008.05756>.
- [19] R.G. Congalton, A review of assessing the accuracy of classifications of remotely sensed data, *Remote Sens. Environ.* 37 (1) (1991) 35–46, [https://doi.org/10.1016/0034-4257\(91\)90048-B](https://doi.org/10.1016/0034-4257(91)90048-B).
- [20] S.B. Patil, S.K. Bodhe, Leaf Disease Severity Measurement Using Image Processing, *Int. J.* 3 (5) (2011) 297–301.
- [21] A.A. Ahmed, G.H. Reddy, A Mobile-Based System for Detecting Plant Leaf Diseases Using Deep Learning, *AgriEngineering* 3 (3) (2021) 478–493, <https://doi.org/10.3390/agriengineering3030032>.
- [22] J. Lu, L. Tan, H. Jiang, Review on convolutional neural network (CNN) applied to plant leaf disease classification, *Agriculture (Switzerland)* 11 (8) (2021) 1–18, <https://doi.org/10.3390/agriculture11080707>.